30

Beyond the SVZ expansion

30.1 Tachyonic gluon mass

We have extensively discussed power corrections related to the IR regions, where the physical picture is simply the increase of the running coupling at large distance. Unconventional $1/Q^2$ corrections which go beyond this simple picture have been also analysed in the literature [161,162,342,341,329,344]. A lattice calculation of [487] shows that the $1/Q^2$ correction arises within a dispersive approach or from a removal of the Landau pole of the running coupling [162,488]. We have sketched this point when presenting the UV renormalons in the previous chapter. Following the presentation in [162], the leading UV renormalon gives the series expansion:

$$F = \left(\sum_n a_n \alpha_s(Q^2) \right)_{UV} = \sum_n n!(-b_0)^n \alpha_s^n(Q^2) \,. \tag{30.1}$$

Using its Borel transform, one has the integral representation:

$$\mathcal{B}[F] = \int dz \, \exp(-z) \frac{(\alpha_s b_0 z)^N}{1 + \alpha_s b_0 z} \,, \tag{30.2}$$

where $N = 1/b_0 \alpha_s$ is the value of n for which the absolute value of the terms reaches its minimum. The integral is of the form:

$$\left(a_n \alpha_s^n(Q^2) \right)_{n=N} \simeq \frac{1}{2} \frac{\Lambda^2}{Q^2} \,, \tag{30.3}$$

where one can notice that the correction comes from the large virtual momenta $p^2 \sim Q^2 \exp(N)$, which is very different with the case of IR renormalon. However, in a theory such as lattice, which possesses an intrinsic UV cut-off, this effect can be irrelevant. Therefore, the alternative dispersive approach of the coupling can be used. The coupling can be parametrized as:

$$\frac{1}{\ln Q^2/\Lambda^2} \rightarrow \frac{1}{\ln Q^2/\Lambda^2} - \frac{\Lambda^2}{Q^2 - \Lambda^2} \,. \tag{30.4}$$

This modification can be justified if one argues that at finite order of perturbation theory the coupling satisfies dispersion relations with cuts at physical $s > 0$. More explicitly, one

329

has:

$$\sum_n a_n \alpha_s(Q^2) \to \sum_n a_n \alpha_s(Q^2) - \sum_n a_n n! b_0^n \frac{\Lambda^2}{Q^2} \ . \tag{30.5}$$

In the case:

$$a_n = n!(-b_0)^n \ , \tag{30.6}$$

the power correction in the second term is still poorly defined. Taking its Borel transform, one obtains:

$$\left(\sum_n (-1)^n \frac{\Lambda^2}{Q^2} \right)_{\text{Borel}} = \frac{1}{2} \frac{\Lambda^2}{Q^2} \ , \tag{30.7}$$

showing that the power corrections from the procedures in Eqs (30.2) and (30.5) are the same, which may indicate that the Borel summation of the UV renormalon series and the removal of the Landau pole from dispersion relation can be intimately connected.

Another issue is the short distance ($r \ll \Lambda$) modification of the QCD potential, which becomes (k is the string tension):

$$\lim_{r \to 0} V(r) = -C_F \frac{\alpha_s(r)}{r} + kr \ , \tag{30.8}$$

while in standard QCD, the leading power correction at short distance is r^2. This leads to the introduction of new small-size non-perturbative corrections and of a new picture of the QCD vacuum. In [161] one discusses this modification of the standard picture in terms of the phenomenology of the tachyonic gluon mass which is assumed to mimic the short-distance non-perturbative effects of QCD. We have seen previously that the $1/Q^2$ corrections to DIS can be explained from the IR region and is consistent with the OPE. In this picture, the constant term of the linear correction can be expressed as [162]:

$$k \approx -\frac{4}{6} \alpha_s \lambda^2 \ , \tag{30.9}$$

where $\lambda^2 < 0$ is the tachyonic gluon mass. In this framework, the standard picture of the OPE within the SVZ expansion gets modified due to the presence of the new $1/Q^2$ term. A systematic evaluation of this contribution using Feynman diagrams has been developed in CNZ. For the current–current two-point functions, it corresponds, to lowest order in α_s, to the evaluation of the diagram in Fig. 30.1.
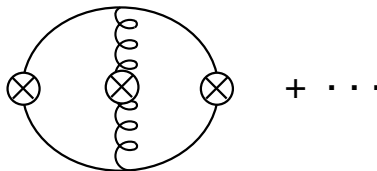

Fig. 30.1. Lowest order diagram contributing to $1/Q^2$. The cross in the gluon propagator corresponds to the tachyonic gluon mass insertion λ^2.

The value of the tachyonic gluon mass has been extracted phenomenologically using previous analysis in [341,329] from e^+e^- data. Analyses of some other channels by CNZ have confirmed such findings. The pion and ρ meson channels give the intersection range:

$$(\alpha_s/\pi)\lambda^2 \simeq -(0.06 \sim 0.07)\,\text{GeV}^2 \,, \quad \text{or} \quad \lambda^2(1.25\,\text{GeV}^2) \approx -(0.34 \sim 0.52)\,\text{GeV}^2 \,, \tag{30.10}$$

leading to the value of the string tension:

$$\sqrt{k} \simeq (369 \pm 14)\,\text{MeV} \,, \tag{30.11}$$

in agreement with the lattice results. The consequences of this result in some paradoxical QCD spectral sum rules channels have been also studied by CNZ, and lead to a resolution of different puzzles for the sum rule scales. One finds, for instance, for these scales:

$$M_\pi^2 \simeq 4M_\rho^2 \,, \tag{30.12}$$

in agreement with the expectations of [382]. Analogous expectations in the gluonium channel has been also recovered. However, this change in the scale does not affect the predictions on the QCD parameters from the sum rules (quark mass, . . .).

30.2 Instantons

Instanton–anti-instanton singularities occur for $b = 4\pi$ in the positive real axis [375]. They occur because far-separated instanton–anti-instanton pairs cannot be properly treated in a perturbative expansion around $\alpha_s = 0$. Due to graph counting rules, perturbation theory has a singularity at $b = 4\pi$, such that perturbation theory alone cannot give an unambiguous answer to the Borel integral for $b > 4\pi$. However, the singularity at $b = 4\pi$ in perturbation theory should also appear in the valley method for instanton-anti-instanton pairs. In addition, a proper definition of $\tilde{\mathcal{D}}(b)$ for $b > 4\pi$, including non-perturbative and non-analytic terms in b should also emerge from the valley method.

In QCD, one expects an important rôle of the instantons due to the topologically non-trivial fluctuations of the gauge fields [381,264], where they are expected to explain the large mass of the η' compared with the usual pseudoscalar mesons [262–264].

30.2.1 't Hooft instanton solution

For a pedagogical introduction, let us start from the example of the Riemann integral (see e.g. [51]):

$$\mathcal{I} = \int_{-\infty}^{+\infty} F(x)e^{-\lambda(x)}dx \,, \tag{30.13}$$

where $\lambda(x)$ is some positive-definite functions. If $\lambda(x)$ has a minimum at the position x_0, one can approximate this function by:

$$\lambda(x) \simeq \lambda_0 + \frac{\lambda''}{2}(x - x_0)^2 + \cdots, \tag{30.14}$$

and obtain:

$$\mathcal{I} \simeq F(x_0)e^{-\lambda_0}\sqrt{\frac{2\pi}{\lambda''}} \ . \tag{30.15}$$

If instead, $\lambda(x)$ has several minimas $\lambda_{0,i}$ at positions $x_{0,i}$, one can approximately write:

$$\mathcal{I} \simeq \sum_i F(x_{0,i})e^{-\lambda_{0,i}}\sqrt{\frac{2\pi}{\lambda_i''}} \ . \tag{30.16}$$

A similar procedure can be done in the evaluation of a functional integral. If the action $S[\Phi]$ has a minimum for a field $\Phi_0(x)$, then this field gives a classical contribution to the functional integral analogously to Eq. (30.15):

$$\int F[\Phi]\mathcal{D}\Phi \sim F[\Phi_0]e^{-S[\Phi_0]} \ , \tag{30.17}$$

where corrections to this result are quantum corrections. If the field $\Phi_0(x)$ leads to a minimum of the action $S[\Phi]$, it is a solution of the Euler–Lagrange equations for that action. Hence solutions of the classical equations of motion lead to classical contributions to the functional integral in Eq. (30.17). There exist classical solutions of pure $SU(2)$ Yang–Mills theory which can be embedded in any $SU(N)$ gauge theory, which are called instantons. The *'t Hooft instanton* solution of the Yang–Mills equation is [264]:

$$G^a_{\mu\nu} = \frac{4\eta^a_{\mu\nu}\rho^2}{g[(x-x_0)^2 + \rho^2]^2} \ , \tag{30.18}$$

where x_0 is the instanton position and $\eta^a_{\mu\nu}$ is the t'Hooft anti-symmetric symbol with the properties:

$$\begin{aligned}
\eta^a_{\mu\nu} &= \epsilon^a_{\mu\nu} \quad \text{for} \quad \mu, \ \nu = 1, 2, 3 \\
\eta^a_{4\nu} &= -\delta^a_\nu \\
\eta^a_{4\mu} &= \delta^a_\mu \\
\eta^a_{44} &= 0 \ ,
\end{aligned} \tag{30.19}$$

where ϵ_{ijk} is the totally anti-symmetric tensor in three-dimensions, while $a = 1, 2, 3$ for the (subgroup) $SU(2)$. The *anti-instanton* solution is obtained by replacing $\eta^a_{\mu\nu}$ by its dual:

$$\tilde{\eta}^a_{\mu\nu} = (-1)^{\delta_{\mu 4} + \delta_{\nu 4}}\eta^a_{\mu\nu} \ . \tag{30.20}$$

In Euclidian space–time, these solutions would correspond to particles of size ρ at a position x_0, while in Minkowskian space–time, the solutions are not particles but can be considered as contributions to the tunnelling between different vacua. The action corresponding to the solution in Eq. (30.18), is easily obtained:

$$\mathcal{S}[G^a]_{cl} = -\frac{1}{4g}\int d^4x \ G^a_{\mu\nu}G^{\mu\nu}_a = \frac{8\pi^2}{g^2} \ . \tag{30.21}$$

The instanton fields are self-dual:

$$\tilde{G}^a_{\mu\nu} = \frac{1}{2}\epsilon_{\mu\nu\alpha\beta}G^a_{\alpha\beta} = G^a_{\mu\nu} \ . \tag{30.22}$$

The action of a self-dual field configuration is determined by its topological charge defined as:

$$Q = \int d^4x \ \left(\frac{g^2}{32\pi^2}\right)G^a_{\mu\nu}\tilde{G}^{\mu\nu}_a \ , \tag{30.23}$$

where an instanton has topological charge $+1$, and an anti-instanton -1. According to Eq. (30.17), the contribution of a single instanton to the vacuum expectation value of the functional $F[G]$ of $G^a_{\mu\nu}$ is:

$$F[G]e^{-S[G]} = F[G]e^{-\frac{8\pi^2}{g^2}} \ . \tag{30.24}$$

From Eqs. (30.21) and (30.24), one can deduce that instantons give genuine non-perturbative contributions, since the exponential cannot be expanded in a convergent power series of g and its asymptotic expansion in g is identically zero.

30.2.2 Instanton phenomenology

Qualitative estimates of the instanton effects based on the dilute gas approximation have been done in the literature [382–385], while an instanton liquid model has also been proposed [386]. However, the results obtained in these papers, for example, for the pseudoscalar quark currents are controversial, which come mainly from the uncontrolled use of the chiral symmetry-breaking parameters entering the analysis. Indeed, one does not know exactly if one should use the light quark current masses or the quark condensate. Moreover, the effects depend also crucially on the size of the instanton, whose value is very inaccurate. In practice, in this model, the instantons contribute as operators of dimension larger or equal than 9–11. For $Q^2 \geq 1$ GeV^2, no appreciable evidence of these effects has been detected in the phenomenological analysis, (even in the pseudoscalar channel, where one often claims that the effects are important!), as we shall see later on. A quantitative estimate of these effects from $e^+e^- \rightarrow I = 1$ hadrons data indeed shows that they are small [387,329], as expected from [385]. A program for measuring instanton induced hard scattering processes at HERA has been proposed [388]. In DIS, one expects to probe small-size instantons, which, in principle, are calculable, where the cross-section behaves as the square of the instanton density $D \sim e^{-\frac{2\pi}{\alpha_s}}$ times a function $F(\epsilon = \sqrt{s}/Q')$ of the total energy over the invariant mass of the particle produced:

$$\sigma \sim e^{-\frac{4\pi}{\alpha_s}F(\epsilon)} \ . \tag{30.25}$$

30.2.3 Dilute gas approximation

In principle, the superposition of two instanton solutions will not be a solution of the Euler–Lagrange equations, due to the non-linearity of these equations for a non-Abelian

gauge theory. If one considers two far-away solutions, the superposition should be a good approximation for two instanton solutions (topological charge 2). In the dilute gas instanton approximation (DIGA), the instanton contribution can be estimated very roughly [382]. In so doing, one starts from the dilute gas density:

$$d(\rho) \approx C \left(\frac{2\pi}{\alpha_s(\rho)} \right)^6 \exp\left(\frac{-2\pi}{\alpha_s(\rho)} \right) : \quad C \approx 0.06 \quad \text{for QCD} , \quad (30.26)$$

where ρ is the instanton radius. Using the previous t'Hooft instanton solution of the Yang–Mills equation the gluon condensates of $2n$ dimensions can be represented as:

$$\langle \mathcal{O}_{2n} \rangle \equiv \left\langle \left(g G^a_{\mu\nu} \right)_1 \cdots \left(g G^a_{\mu\nu} \right)_n \right\rangle = \int_0^{\rho_c} d\rho \, \frac{d(\rho)}{\rho^{2n+1}} , \quad (30.27)$$

where ρ_c is the critical cut-off size of the instanton. By introducing the approximate relation:

$$\frac{2\pi}{\alpha_s(\rho)} \approx \frac{2\pi}{\alpha_s(\rho_c)} + 11 \log(\rho_c/\rho) , \quad (30.28)$$

one obtains:

$$\begin{aligned} \langle \mathcal{O}_{2n} \rangle \approx & \frac{1}{(11 - 2n)} \frac{1}{\rho_c^{2n}} \left(\frac{2\pi}{\alpha_s(\rho_c)} \right)^6 \exp\left(-\frac{2\pi}{\alpha_s(\rho_c)} \right) \\ & \times \sum_{k=0}^6 \frac{6!}{(6-k)!} \left(\frac{11}{2(11-2n)} \alpha_s(\rho_c) \right)^k , \end{aligned} \quad (30.29)$$

indicating that, for condensates of a critical dimension:

$$2n = 11 , \quad (30.30)$$

one has a phase transition which separates the large-size instantons ($2n \leq 11$), that is, *ordinary low-dimension* condensates, with the small-size instanton (*instanton–anti-instanton or one-instanton*) effects. As emphasized in the previous derivation, the small-size instanton is very sensitive to the value of the instanton radius ρ_c, which renders (among many other unknown) uncertain the quantitative estimate of its effect. Some other reasons, as we shall see below are the inconsistency of the size and distance between instanton ensembles. For these different reasons, the estimate based on DIGA should only be considered at the qualitative level. Using the general expression in Eq. (30.29) for estimating, the contribution of the instanton to the NP gluon condensate $\langle g^2 G^2 \rangle$, and using the value of $\alpha_s(\rho_c) \approx 1$, one can deduce:

$$\langle g^2 G^2 \rangle_{\text{inst}}^{1/4} \geq \frac{4}{\rho_c} . \quad (30.31)$$

Using the previous expression of the topological charge and the self-duality relation, one obtains for n_d dilute instantons in a volume V greater than the instanton size, the instanton

density:[1]

$$n_0 \equiv \frac{n_d}{V} = \frac{1}{V} \int_V Q(x) d^4x = \frac{1}{32\pi^2} \langle g^2 G^2 \rangle_{\text{inst}} . \tag{30.32}$$

Therefore the average distance d_I between two instantons is:

$$d_I \equiv n_0^{-1/4} = \left(\frac{32\pi^2}{2\langle g^2 G^2 \rangle_{\text{inst}}} \right)^{1/4} . \tag{30.33}$$

These two equations give the ratio:

$$\frac{d_I}{\rho_c} \leq 0.7 , \tag{30.34}$$

which is smaller than 1. It may indicate that the dilute gas approximation is inconsistent, or it can indicate that higher unknown perturbative corrections or non-perturbative contributions (multi-instantons) to the classical result are important. Alternatively, one can integrate the tunnelling rate in order to get the phenomenological value of the instanton density [389]:

$$n_{\text{phen}} = \int_0^{\rho_c} d\rho \; n_0(\rho) , \tag{30.35}$$

which for $n_{\text{phen}} = 1 \text{ fm}^{-4}$, gives $\rho_c = 1$ fm using the SVZ value of the gluon condensate, which is rather pessimistic.[2]

30.2.4 The instanton liquid model

A more promising picture is the instanton liquid model [386,390]. The non-perturbative contribution to the instanton density defined previously can be estimated from the gluon condensate. The interaction of an instanton with an arbitrary external field $G_{\mu\nu}^a$ is:

$$S_{\text{int}} = \frac{2\pi^2 \rho^2}{g^2} \bar{\eta}_{\mu\nu}^a U^{ab} G_{\mu\nu}^b , \tag{30.36}$$

which is a dipole interaction, and then does not contribute to the average action to first order. U is an unitary matrix describing the orientation of the instanton in colour space. One can deduce [391]:

$$n(\rho) = n_0(\rho) \left[1 + \frac{\pi^4 \rho^4}{2g^4} \langle G^2 \rangle + \cdots \right] , \tag{30.37}$$

which has been exponentiated by [392]. In this way, and using $n_{\text{phen}} = 1$ fm, one obtains using the SVZ value of the condensate:

$$\rho_c = 1/3 \text{ fm} , \tag{30.38}$$

---

[1] In the classical field approach, the quantity below has no g^2 factor.
[2] However, the SVZ value of the gluon condensate has been underestimated by a factor of about 2 [329,313] such that the value of ρ_c becomes 0.5 fm which leads to a more optimistic situation.

which is rather small. This result gives a different picture of the QCD vacuum. The instanton size being smaller than the separation between instantons implies that the vacuum is dilute. Also, the field inside the instanton is very strong:

$$G_{\mu\nu} \gg \Lambda^2 \,, \tag{30.39}$$

implying that the semi-classical approximation is valid. The action is large:

$$S = 8\pi^2/g^2 \sim 10 - 15 \gg 1 \,. \tag{30.40}$$

Also, instantons retain their individuality and are not destroyed by interactions:

$$\delta S_{\text{int}} \ll S_0 \,, \tag{30.41}$$

while interactions are important for the structure of the instanton ensemble:

$$(\exp |\delta S_{\text{int}}| \sim 20 \gg 1) \,. \tag{30.42}$$

The phenomenology of the instanton liquid model has been published in [386], which readers can consult for more details.

30.3 Lattice measurements of power corrections

Recent lattice measurements of the $V \pm A$ and (pseudo)scalar (S, P) two-point correlators have been done in [393] in the x-space and have been compared with different models of power corrections (SVZ, ILM). Using the expressions of the correlators in the momentum space given in the previous section, and using the Fourier transform formulae in Table G.1 from [394] given in Appendix G, the different QCD expressions of the $V + A$ and $S + P$ correlators of interest here[3] in the x-space normalized to the perturbative contributions are [394]:

$$\frac{\Pi^{V+A}}{\Pi^{V+A}_{\text{pert}}} \rightarrow 1 - \frac{\alpha_s}{4\pi}\lambda^2 \cdot x^2 - \frac{\pi}{48}\langle\alpha_s(G^a_{\mu\nu})^2\rangle x^4 \ln x^2 + \frac{2\pi^3}{81}\alpha_s\langle\bar{q}q\rangle^2 x^6 \ln x^2 \,, \tag{30.43}$$

where we adopt the convention $\ln x^2 < 0$. We have added to the usual SVZ-expansion the quadratic x^2 correction from [161]. In the $V - A$ channel, the usual SVZ expansion works quite well but for a small radius of convergence. In the $V + A$ channel, the SVZ-expansion as well as the ILM describe quite well the quantity $Q^2\Pi(Q^2)$, which is expected not to have a $1/Q^2$-term [161]:

$$\frac{Q^2 \cdot \Pi^{V+A}}{Q^2 \cdot \Pi^{V+A}_{\text{pert}}} \rightarrow 1 - \frac{\pi}{96}\langle\alpha_s(G^a_{\mu\nu})^2\rangle x^4 + \frac{2\pi^3}{81}\alpha_s\langle\bar{q}q\rangle^2 x^6 \ln x^2. \tag{30.44}$$

This is to be contrasted to the case of $\Pi(Q^2)$, which needs also to be measured on the lattice, in order to test the existence of the $1/Q^2$ in the $V + A$ channel. However, the channel

---

[3] Some other correlators in the x-space are given in Chapter 39.

Table 30.1. *Different parameters used in the analysis of the S + P data in units of GeV^d (d is the dimension of the operator)*

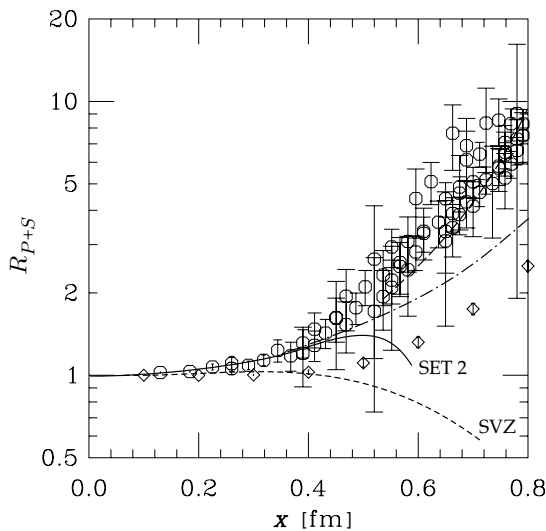| Sources	$\langle \alpha_s G^2 \rangle$	$\alpha_s \langle \bar{\psi}\psi \rangle^2$	$(\alpha_s/\pi)\lambda^2$
SET 1 (SVZ) [1]	0.04	0.25^6	0
SET 2 [313,329]	0.07	5.8×10^{-4}	0
SET 3 [313,329,161]	0.07	5.8×10^{-4}	-0.12

Fig. 30.2. *S + P* channel: comparison of the lattice data from [393] with the OPE predictions for the two sets of QCD condensate values given in Table 30.1 . The dot-dashed curve is the prediction for SET 3 where the contribution of the x^2-term has been added to SET 2. The bold dashed curve is SET 3 + a fitted value of the $D = 8$ condensate contributions. The diamond curve is the prediction from the instanton liquid model of [386].

which is crucial for the present analysis is the $(S + P)$ one. In this channel:

$$R_{P+S} \equiv \frac{1}{2}\left(\frac{\Pi^P}{\Pi^P_{\text{pert}}} + \frac{\Pi^S}{\Pi^S_{\text{pert}}} \right)$$

$$\rightarrow 1 - \frac{\alpha_s}{2\pi}\lambda^2 x^2 + \frac{\pi}{96}\langle \alpha_s (G^a_{\mu\nu})^2 \rangle x^4 + \frac{4\pi^3}{81}\alpha_s \langle \bar{q}q \rangle^2 x^6 \ln x^2 . \quad (30.45)$$

As shown in Fig. 30.2, neither the SVZ-expansion nor the ILM can describe the lattice data, where we have used the sets of condensate values given in Table 30.1.

If such data are confirmed, it may indicate a strong evidence of the quadratic $1/Q^2$ power correction. We can see in Fig. 30.2, that for large x, the data is better fitted by including
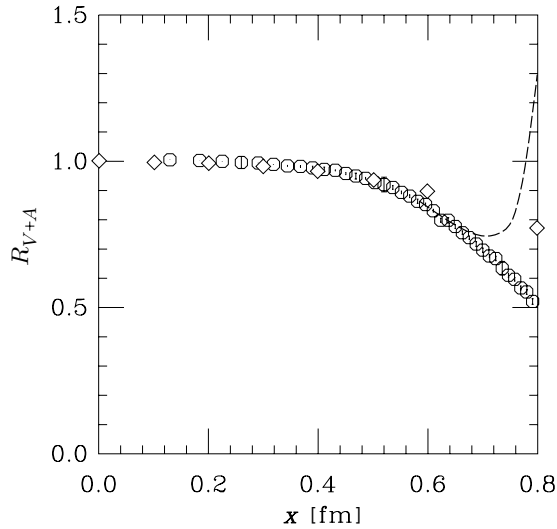
Fig. 30.3. $V + A$ channel: comparison of the lattice data from [393] with the OPE predictions for the SET 3 QCD condensates values given in Table 30.1 including a fitted value of the $D = 8$ contributions. The diamond curve is the prediction from the instanton liquid model of [386].

both the $1/Q^2$ correction and a $D = 8$ dimension condensates where the latter differ notably from the vacuum saturation estimate, with the size:

$$C_8 \mathcal{O}_8 \simeq + \left(\frac{x}{0.58}\right)^8 , \tag{30.46}$$

compared with the one from a modified vacuum saturation [399,411]:

$$C_8 \mathcal{O}_8|_{\text{fac}} \simeq + \frac{3395}{30855168} \langle \alpha_s G^2 \rangle^2 x^8 \approx \left(\frac{x}{1.2}\right)^8 . \tag{30.47}$$

For completeness we also show in Fig. 30.3, a fit of the $V + A$ channel including the $D = 8$ condensate contributions. One can notice that like in the case of the $S + P$ channel, the value of the $D = 8$ condensates differs notably from the vacuum saturation estimate. It reads:

$$C_8 \mathcal{O}_8 \simeq + \left(\frac{x}{0.7}\right)^8 , \tag{30.48}$$

compared with the one from a modified vacuum saturation [399,411]:

$$C_8 \mathcal{O}_8|_{\text{fac}} \simeq + \frac{2}{3428352} \langle \alpha_s G^2 \rangle^2 x^8 \approx \left(\frac{x}{2.5}\right)^8 . \tag{30.49}$$

One can conclude from the lattice measurement of the $S + P$ correlators that, if the data have to be explained by power corrrections, it can only be done by the presence of λ^2 quadratic corrections at moderate distance (less than 0.5 fm). For larger distances, one needs to add the contributions of higher eight-dimension condensates. It has been

argued [395] that the λ^2 correction can be better understood within the effective Higgs-like theories which are common within the monopole mechanism of confinement, where, in the presence of a magnetically charged (effective) scalar field, the symmetry of the theory is $SU(3)_{\mathrm{colour}} \times U(1)_{\mathrm{magnetic}}$. Upon the spontaneous breaking of the magnetic $U(1)$ the gauge boson acquires a non-vanishing mass and its mass squared is the only parameter of dimension $d = 2$ consistent with the symmetry. Moreover, in exchanges between (colour) charged particles the gauge-boson mass appears to be the tachyonic mass as was demonstrated on the $U(1)$ example in [396,397]. Detailed analysis of various power corrections within the Higgs-like models can be found in [396–398]. Moreover, if the monopole size is indeed as small as indicated above, then the effective Higgs-like theories can apply at all distances $\sim (0.1 \div 0.5)$ fm.